Photothermal radiometric investigation of implanted silicon: The influence of dose and thermal annealing

Andreas Othonos, Constantinos Christofides,[a] and Andreas Mandelis[b]
Department of Natural Sciences, Faculty of Pure and Applied Sciences, University of Cyprus, P.O. Box 537, 1678 Nicosia, Cyprus

(Received 12 April 1996; accepted for publication 29 May 1996)

Photothermal radiometric measurements were performed on phosphorus implanted and annealed silicon wafers. Data were collected over modulation frequencies ranging between 0.1 and 100 kHz with the 488 nm Ar ion laser line as the excitation source. The sensitivity of this technique on implantation dose and annealing temperature is discussed. A semiquantitative analysis of the data is also carried out. © *1996 American Institute of Physics.* [S0003-6951(96)04432-4]

Ion implantation is a key technological process in modern microelectronics which was introduced as an alternative to diffusion for the semiconductor doping process.[1,2] However, some disadvantages result from ion implantation such as damage into the semiconductor due to the energetic character of the process. The consequence of this bombardment is the amorphization of the semiconductor surface and the presence of electrical defects such as interstitials, dislocations, grain boundaries, or inhomogeneities.[1,2] Therefore, ion implantation has to be followed by an annealing process in order for the semiconductor to recover its crystallinity and for the doping impurity to become active.[3]

Since the mid-1980's various photothermal techniques have been developed for the characterization of implanted materials.[4] The non-contact character of the thermal wave techniques makes them particularly attractive for nondestructive evaluation (NDE) of materials.[4,5] Photothermal radiometry (PTR), which allows the measurements of the optically induced emission of blackbody radiation at the surface of a semiconductor,[6–9] is a powerful technique for the characterization of implanted wafers. It was found that the residual damage in the lattice reduces the photothermal radiometric signal level from the sample under certain conditions. With this technique one can deduce information concerning the amorphization level of the implanted layer through the band-to-band and/or band-to-impurity level recombination time and the surface recombination velocity. A significant advantage of PTR of semiconductors over pump/probe photomodulated thermoreflectance (PMTR) detection,[10] is the observation[11] that, with relatively low impurity concentrations, the PTR signal is strongly dominated by the dynamics of the photoexcited carrier plasma recombination.

In this letter we present experimental results on the influence of implantation dose on the PTR signal, as well as the influence of the annealing temperature. All photothermal radiometric measurements in this work have been obtained using apparatus similar to the one employed in the past.[6–9] Experimental data obtained from PTR measurements on phosphorus implanted silicon are presented. Silicon wafers, lightly doped with boron ($\rho \approx 20$–$25\ \Omega$ cm), were implanted with phosphorus at various doses Φ at 150 keV (W1-W6, see description in Fig. 1). The phosphorus ion implantation was performed through a thin oxide layer at room temperature. Some samples were then annealed isochronally for 1 h at various temperatures ranging from 300 to 1100 °C in N_2 atmosphere. After annealing, the oxide overlayer was etched away and the samples were used for the experiments. The same series of samples has been used for PMTR measurements by Seas and Christofides.[12]

Figure 1 presents the variation of the PTR signal amplitude as a function of the modulation frequency for various implantation doses (samples: W1-W6) for the non-annealed samples. We generally note a decrease of the PTR amplitude (especially at low frequencies) with increasing implantation dose. The trend, however, is not monotonic, especially for samples W4-W6. Similar phenomena were also observed in the past by Sheard *et al.*[6,8] To understand this behavior we can use the simple relation given by Sheard *et al.*[11]

$$\Delta q = \frac{\eta I_o (1-R)}{h\nu\sigma(D\sigma + s)}, \tag{1}$$

Δq is the PTR signal, η is the photocarrier generation efficiency, and R is the surface reflectivity; I_o is the beam intensity; $h\nu$ is the photon energy; s is the surface recombina-

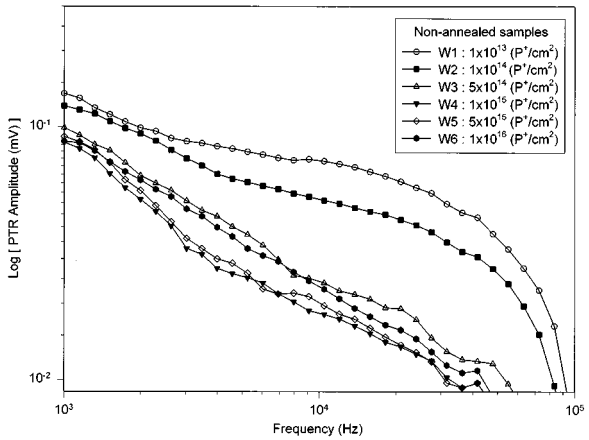

FIG. 1. Photothermal radiometric amplitude vs modulation frequency for non-annealed samples implanted at the various implantation doses of Table I.

[a]Electronic mail: costasc@earth.ns.ucy.ac.cy
[b]On leave from the Photothermal and Optoelectronic Diagnostics Laboratory, Department of Mechanical Engineering, University of Toronto, Toronto M5S 3G8, Canada. Electronic mail: mandelis@mie.utoronto.ca

tion velocity; D is the ambipolar diffusion coefficient; and σ is the complex plasma-wave propagation coefficient given by

$$\sigma = \frac{1 + j\omega\tau}{D\tau}, \tag{2}$$

with ω being the angular modulation frequency and τ the carrier recombination lifetime. Taking logarithms we obtain

$$\log_{10}|\Delta q(\omega)| \propto A - \log_{10}\left[\left(\frac{1 + j\omega\tau}{\tau}\right)(1 + U)\right], \tag{3}$$

where U is given by

$$U = \frac{s\tau}{L_e\sqrt{(1 + j\omega\tau)}}, \tag{4}$$

A is a normalization constant, and L_e is the injected carrier diffusion length, $L_e = \sqrt{D\tau}$. In general, in the case of implanted silicon U can be ignored for the working modulation frequencies 0.1–100 kHz utilized in the present experimental work: U was calculated for pure silicon ($\tau = 4 \times 10^{-4}$ s, $s = 10$ cm/s, and $D = 18$ cm^2/s)[13] and for highly implanted and amorphous silicon ($\tau = 1 \times 10^{-8}$ s, $s = 10^4$ cm/s, and $D = 1$ cm^2/s).[14] Thus, at low frequencies, $\omega\tau \ll 1$, and the above relation becomes equal to $A + \log_{10}\tau$, independent of ω for both cases. From this relation it is now obvious that at low frequencies an increase of τ leads to an increase of the photothermal radiometric signal. On the other hand at high frequencies where $\omega\tau \gg 1$, Eq. (3) approaches $A + \log_{10}(j\omega + 1/\tau + (s/\sqrt{D})\sqrt{(1/\tau) + j\omega})$. For long recombination lifetimes, so that $\omega\tau \gg 1$, this expression approximately becomes $A + \log_{10}(j\omega + (s/\sqrt{D})\sqrt{j\omega})$. The slope of the curve is determined by the material parameter ratio $s/\sqrt{D}$. For short τ, so that $\omega\tau \ll 1$, the foregoing expression becomes $A + \log_{10}(1/\tau + s/L_e)$, independent of ω. These remarks explain the PTR signal amplitude decrease with increasing implantation dose, as the results of a decrease of the carrier lifetime. Furthermore, in Fig. 1 one can distinguish two groups of curves: one group which contains the slightly implanted wafers (W1 and W2) and another group with heavier implantation around the critical amorphization dose (W3-W6). The foregoing discussion also indicates that the carrier surface recombination velocities and electronic diffusivities are similar for wafers W1 and W2 where $\omega\tau \geqslant 1$ is expected. On the other hand it is expected that $\omega\tau \ll 1$ for the wafers W3-W6, yielding high-frequency slopes essentially independent of ω. The frequency-dependent negative slopes of the PTR amplitudes of Fig. 1 are due to the thermal-wave component.[15] This component is additive to the plasma-wave response and appears dominant at low frequencies in curves W1 and W2, and at low frequencies in curves W3-W6, consistent with the increased degree of damage in the latter. The implantation-induced deterioration of the near-surface thermophysical properties of samples W5, W6 appears to be severe, resulting in the localization of the thermal-wave centroid and an increase in the PTR signal, due to poor heat conduction to the substrate. This reverses the amplitude (i.e., thermal-wave intensity) trend in W5, W6 compared to samples W3 and W4.

Figure 2 presents the variation of the PTR signal amplitude for the highest annealed samples W1-W6 (1100 °C) as a function of the modulation frequency for various implantation doses. The signal is almost one order of magnitude higher than that obtained from the non-annealed samples. Again, this can be explained by the fact that in the annealed samples the plasma-wave mechanisms is partially or totally restored, which leads to higher signals. In this case the slightly implanted wafers W1-W2 exhibit the independence from the modulation frequency for $f \leqslant 5 \times 10^4$ Hz, expected from low-frequency plasma waves, Eq. (2), with a similar downturn rate at higher frequencies signifying similar values of the parameter $s/\sqrt{D}$. On the other hand the annealing of the more heavily implanted wafers W3-W6 was incomplete, as they still exhibit a thermal-wave decay envelope throughout the entire frequency range. The high-frequency downturn signifies similar values for $s/\sqrt{D}$ for their group. In both Figs. 1 and 2 we note that for each frequency the PTR signal of wafer W6 is lower than the one of wafer W5 which was implanted at a lower dose. This is due to self-annealing, as was recently reported.[12,16]

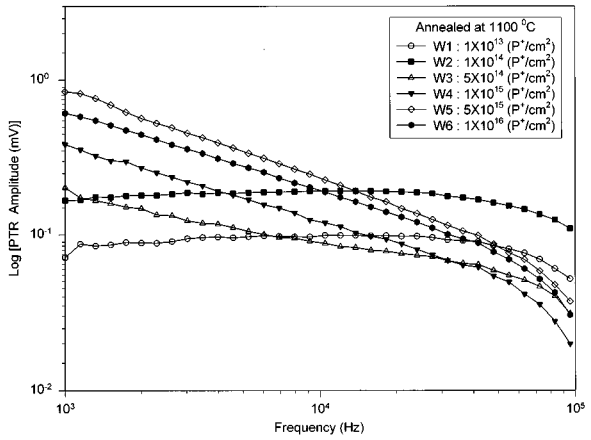

FIG. 2. Photothermal radiometric amplitude vs modulation frequency for highly annealed (1100 °C) samples implanted at the various doses of Table I.

Figure 3 presents the PTR signal amplitude as a function

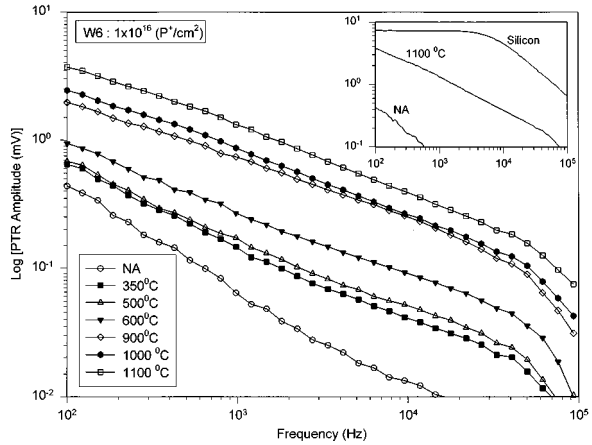

FIG. 3. Photothermal radiometric amplitudes vs modulation frequency for W6-type samples of Table I annealed at various temperatures. Inset: PTR signal amplitude vs frequency for the silicon substrate and two implanted samples.

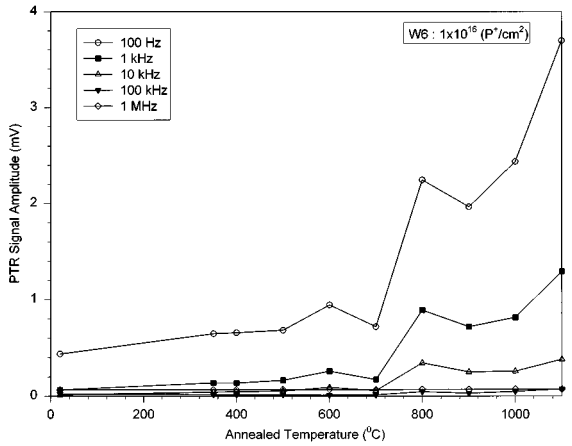

FIG. 4. Photothermal radiometric vs annealing temperature for W6-type samples implanted at 1×10^{16} P^+/cm^2 for various modulation frequencies between 100 Hz and 1 MHz.

of modulation frequency for the W6 series samples. This consists of an unannealed and several annealed samples at various temperatures in the range of 300–1100 °C. The more highly annealed samples exhibit much higher signals than the unannealed and slightly annealed samples. This, again, is consistent with the plasma-wave restoration[15] within a thermal wave ''envelope'' due to residual unannealed damage. The inset of Fig. 3 presents the PTR signal amplitude versus frequency for the silicon substrate and two implanted samples.

Figure 4 presents the variation of the PTR signal versus annealing temperature for various modulation frequencies. It is immediately obvious that the PTR amplitude increases as a function of the annealing temperature, with higher relative increases at low modulation frequencies. On the contrary, in the case of high modulation frequencies (100 kHz and 1 MHz) the radiometric signal amplitude is essentially insensitive to the annealing temperature. This is in agreement with the foregoing interpretation that at low modulation frequencies the PTR signal is directly related to the lifetime, whereas at higher frequencies it is related to the parameter $s/\sqrt{D}$. This parameter is known to have a much narrower range of variation with implantation treatment than τ.[15] In Fig. 4 various regimes of the annihilation process of implanted impurities can be distinguished. A smooth recovery of various types of point defects is evident at the low temperature regime, while an anomaly appears around 600 °C, when a formation of complex defects occurs[3] and this leads to a small decrease of the signal. After the recovery of those complex defects the signal increases drastically up to 800 °C with a new decrease taking place 900 °C. This decrease is probably related to the generation of dislocation loops in the implanted and annealed region.[3] The presence of dislocation lines at this stage has also been observed by Matsumori *et al.*[17] using thermal-wave photoacoustic techniques. Further annealing at higher temperatures results in the disappearance of dislocations and the PTR signal amplitude increases again.

In conclusion, we have shown that the photothermal radiometric technique is a useful and sensitive NDE technique for studying the influence of ion implantation dose as well as the subsequent thermal annealing process of implanted wafers through the relative interplay between plasma and thermal wave mechanisms. In view of this conclusion, it is also important to put in perspective the sensitivity of this technique in comparison with other semiconductor characterization methods: We performed Raman spectroscopy,[16,18] photoluminescence measurements[19] as well as photothermal reflectance measurements on the same series of samples.[12] Comparison of the PTR results with the data obtained with those previously used techniques showed superiority of the sensitivity of the radiometric technique toward monitoring implantation defects including residual damage. A quantitative analysis of the foregoing comparisons will be submitted for publication in the near future.

The support of the French Cultural Center of Cyprus is gratefully acknowledged.

[1] H. Ryssel and I. Ruge, *Ion Implantation* (Wiley, New York, 1986).
[2] G. Ghibaudo and C. Christofides, *Semiconductors and Semimetals* (Academic, New York, 1996), Vol. 45.
[3] C. Christofides, Semicond. Sci. Technol. **7**, 1283 (1992).
[4] *Photoacoustics and Thermal Wave Phenomena in Semiconductors*, edited by A. Mandelis (North-Holland, New York, London, 1987).
[5] C. Christofides and G. Ghibaudo, *Semiconductors and Semimetals* (Academic, New York, 1996).
[6] S. Sheard and M. Somekh, in *Non-Destructive Evaluation, Vol. II, Progress in Photothermal and Photoacoustic Science and Technology*, edited by A. Mandelis (PTR-Prentice Hall, Englewood Cliffs, NJ, 1994), Chap. 5.
[7] A. Seas, C. Christofides, and M. Munidasa, Appl. Phys. Lett. **68**, 538 (1996).
[8] T. M. Hiller, M. G. Somekh, S. J. Sheard, and D. R. Newcombe, Mater. Sci. Eng. B **5**, 107 (1990).
[9] G. M. Crean, S. J. Sheard, C. W. See, and M. G. Somekh, IEEE Ultrason. Symp. (1987).
[10] A. Rosencwaig, J. Opsal, W. L. Smith, and D. L. Willenborg, Appl. Phys. Lett. **46**, 1013 (1985).
[11] S. J. Sheard, M. G. Somekh, and T. Hiller, Mater. Sci. Eng. B **5**, 101 (1990).
[12] A. Seas and C. Christofides, Appl. Phys. Lett. **66**, 3346 (1995).
[13] R. F. Pierret, *Modular Series on Solid State Devices, Vol. VI Advanced Semiconductor Fundamentals*, edited by R. F. Pierret and G. W. Neudeck (Addison-Wesley, Reading, MA, 1987), pp. 188–192.
[14] M. Nestoros, B. C. Forget, C. Christofides, and A. Seas, Phys. Rev. B **51**, 14115 (1995).
[15] A. Mandelis (unpublished).
[16] A. Othonos, C. Christofides, J. B. Said, and M. Bisson, J. Appl. Phys. **75**, 8032 (1994).
[17] T. Matsumori, M. Uchida, T. Izumi, and F. Uehara, *1991 7th International Topical Meeting on Photoacoustic and Photothermal Phenomena, 26–30 August 1991, Doorwerth, The Netherlands*, Conference Digest and Technical Abstracts, pp. 473–474.
[18] A. Othonos and C. Christofides, Nucl. Instrum. Methods B (in press, 1996).
[19] A. Othonos and C. Christofides, J. Appl. Phys. **78**, 796 (1995).